Scientia Iranica A (2016) 23(2), 420–428

SCIENTIA IRANICA

Sharif University of Technology
Scientia Iranica
Transactions A: Civil Engineering
www.scientiairanica.com

Investigations into factors influencing the CBR values of some Aegean sands

Y. Erzin[a,*], D. Türköz[a], Y. Tuskan[a] and I. Yılmaz[b]

a. *Department of Civil Engineering, Celal Bayar University, 45140 Manisa, Turkey.*
b. *Department of Geological Engineering, Cumhuriyet University, 58040 Sivas, Turkey.*

Received 12 March 2014; received in revised form 23 May 2015; accepted 15 September 2015

KEYWORDS
Aegean sands;
California bearing ratio;
Experimental investigations;
Particle morphology;
Multiple regression analysis.

Abstract. The California Bearing Ratio (CBR) value of the soils is very important for geotechnical engineering and earth structures. A CBR value is affected by the soil type and different soil properties. With this in view, in this paper, an attempt has been made for investigating the factors that affect the CBR values of some Aegean sands collected from nine different locations in Manisa (Turkey). The sand samples were tested for mineralogy, particle shape and size, and specific gravity. The CBR tests were then performed on these samples at different dry densities to examine the influence of dry density, relative density, water content, and particle shape and size on the CBR value. Multiple Regression Analysis (MRA) was performed to predict the CBR value of the sands by using the experimental results. Moreover, several performance indices, such as coefficient of correlation and variance account for mean absolute error and root mean square error, were calculated to check the prediction capacity of the proposed MR equation. The obtained indices make it clear that the equation derived from the samples used in this study applies well, with an acceptable accuracy, to the CBR estimation at the preliminary stage of site investigations.

1. Introduction

The California Bearing Ratio (CBR) has been acknowledged as a significant parameter to characterize the bearing capacity of earth structures, such as earth dams, road embankments, airport runways, bridge abutments, and pavements [1]. The CBR is described as the ratio of force per unit area required to penetrate a soil mass with standard circular piston at the rate of 1.25 mm/min. to that required for the corresponding penetration of a standard material [2]. The CBR tests can be carried out either in the laboratory or in the field [3]. In the laboratory, the CBR test is typically accomplished on compacted soil samples, while in the field, the CBR test is carried out on a ground surface or on a level surface excavated in a test pit, trench, or bulldozer cut [4]. The CBR test results are very valuable for geotechnical engineering and earth structures such as earth dams, highway embankments, bridge abutments, and the fills behind retaining walls [5]. A CBR value is influenced by the type of soil and different soil properties [6]. Many investigators (e.g., [7-21]) have performed studies to demonstrate the influence of soil types and characteristics on the CBR values. The CBR value has also been connected empirically with resilient modulus and a variety of other engineering soil properties [20].

In this paper, an attempt has been made for investigating the factors that affect the CBR value of some Aegean sands, which were collected from nine different locations in Manisa (Turkey), as depicted in Figure 1. These samples were tested for mineralogy, particle shape and size, and specific gravity [22]. The

*. *Corresponding author. Tel.:90 236 2012312; Fax: 90 236 2412143*
E-mail addresses: yusuf.erzin@bayar.edu.tr (Y. Erzin); iyilmaz@cumhuriyet.edu.tr (I. Yılmaz)

Table 1. Physical and compaction characteristics of the sand samples [22].

Sample	G_s	$e_{\max}$	$e_{\min}$	w_{opt} (%)	D_{10} (mm)	D_{50} (mm)	C_u	C_c	Unified soil classification
A	2.68	0.90	0.47	13.9	0.94	1.50	1.92	0.88	SP
B	2.68	0.96	0.56	11.0	0.88	1.23	1.58	0.91	SP
C	3.24	0.75	0.28	12.2	0.17	0.77	5.91	1.39	SP
D	2.67	0.92	0.57	11.8	0.12	0.45	4.76	1.78	SP-SM
E	2.56	0.87	0.51	13.4	0.87	1.26	1.68	0.90	SP
F	2.67	0.90	0.24	2.6	0.29	0.81	3.53	1.12	SP
G	3.57	1.07	0.62	9.9	0.60	1.25	2.53	1.09	SP
H	3.30	1.04	0.54	14.4	0.91	1.39	1.78	0.89	SP
I	2.48	0.76	0.39	7.2	1.51	1.10	2.62	1.10	SP

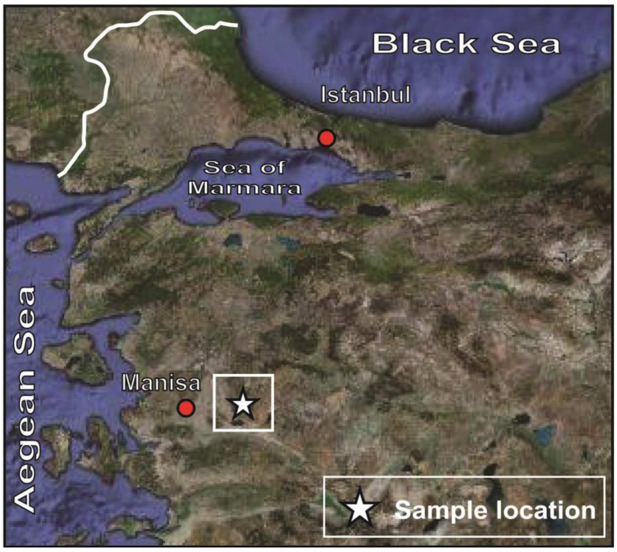

Figure 1. Location map of the study area [22].

CBR tests were then performed on these samples with different dry densities and the influence of dry density, relative density, specific gravity, water content, and particle shape and size on the CBR value was examined [22]. In addition, Multiple Regression Analysis (MRA) has been performed to predict the CBR value of sands by employing the experimental results.

2. Experimental investigations

2.1. Materials

In order to study the factors affecting the CBR value of sands, Aegean sands were collected from nine different locations in Manisa, as depicted in Figure 1 [22]. These sands were air-dried and the fraction passing through a 4.76 mm sieve (ASTM No. 4) was separated into representative sub-samples by passing through the riffle box.

2.2. Physical characteristics of the samples

In order to obtain gradational characteristics of these sands, sieve analyses were performed in duplicate on

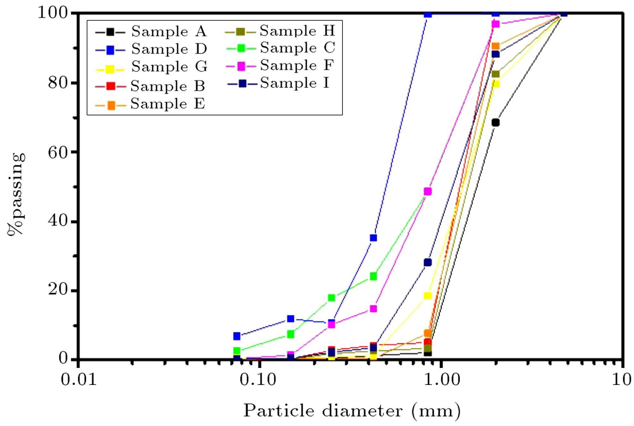

Figure 2. Particle size distribution characteristics of the sand samples [22].

each sample following the guidelines presented by ASTM D 422-63 [23]. The average values were used for developing the representative gradation curve for each sand sample. The gradational curves for the sand samples are given in Figure 2 and the basic soil parameters are presented in Table 1. Specific gravity, G_s, tests were performed according to Turkish Standards (TS1900-1) [24] to determine the G_s values of the samples, and the results are given in Table 1.

The relationship between dry density and water content was determined by using the 2.5 kg rammer method following the Turkish Standards (TS1900-1) [24]. The optimum water content (w_{opt}) is given in Table 1 for each sand sample. Maximum and minimum compaction tests were also performed on each sample (BS1377/Part 4, 1990) [25] to determine the maximum and minimum densities ($\rho_{\max}$ and $\rho_{\min}$). The results of these tests were utilized to calculate the maximum and minimum void ratios ($e_{\max}$ and $e_{\min}$); these ratios are given in Table 1.

2.3. X-ray diffraction analyses

Mineralogical determinations by means of X-ray diffraction analyses were carried out by using whole-rock powder in the Material Laboratory of Izmir

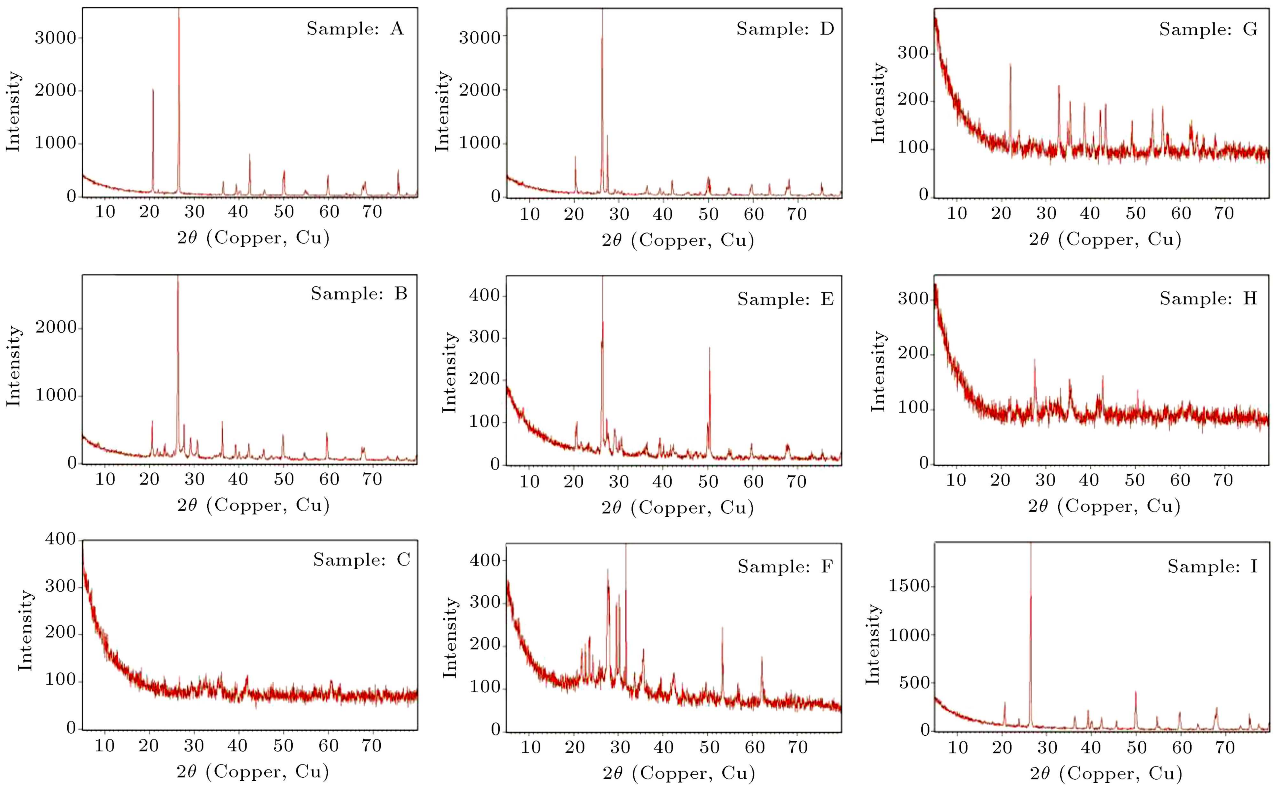

Figure 3. Characteristic XRD diffractograms of the sand samples [22].

Institute of Technology (Izmir-Turkey). The samples obtained from nine different locations were first air-dried and then grinded as powder in a mechanic grinder. The slides were prepared from the powder of both coarse and fine grains, and X-ray diffractograms were obtained for each sample by using the X-ray diffraction techniques (Figure 3). According to the characteristic peaks for each mineral, the composition of minerals and their semi-quantitative quantities were first identified from the X-ray diffractions on whole rock powder. According to XRD results, 100% proportion of quartz was found in Samples A and I. Quartz appeared to be the dominant mineral in Samples B, D, E, and F, while feldspar was the second dominant mineral. Calcite, dolomite, and clay minerals accompanied quartz and feldspar. In Sample H, higher proportions of feldspar minerals were observed, and 25% corundum mineral was also determined. While in Sample G higher proportion of corundum (100%) was observed, Sample C was evaluated as a completely amorphous material (100%). The results of XRD are also summarized in Table 2.

Table 2. Whole rock powder diffraction analysis results (%fraction by weight) for the sand samples [22].

Sample	Q	Fel	Ca	Dol	Px	C	Clay	A
A	100	-	-	-	-	-	-	-
B	60	25	5	5	-	-	5	-
C	-	-	-	-	-	-	-	100
D	60	30	5	-	-	-	5	-
E	55	25	10	5	-	-	5	-
F	60	40	-	-	-	-	-	-
G	-	-	-	-	-	100	-	-
H	-	75	-	-	-	25	-	-
I	100	-	-	-	-	-	-	-

Q: quartz; Fel: feldspar; Ca: calcite; Dol: dolomite; Px: pyroxene; C: corund; and A: amorphous.

2.4. Particle shape analyses

Sedimentologists usually demonstrate the particle shape in connection with surface texture, sphericity, and roundness (e.g. [26,27]). Generally, surface texture is used to define irregularities of the surface of the particles that have too little influence on the overall shape. Sphericity (S_R) is the ratio of the surface area of a sphere having the same volume as that of the soil particle to the surface area of the particle [28]. A sphericity value of 1 implies a perfect sphere and it decreases with irregularity of the particles. Roundness (R_F) is connected with the sharpness of the corners and edges on grain surfaces. In this study, particle shape analyses were carried on 120 grains of each sand sample to determine the S_R and roundness R_F values of each sand sample.

The sphericity (S_R) of the particle of each grain was determined by using the method developed by

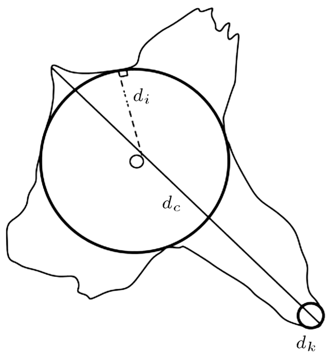

Figure 4. Definitions of angularity and sphericity [30].

Riley [29], represented by Eq. (1):

$$S_R = d_i/d_c, \tag{1}$$

where, d_c is the diameter of the circumscribing circle (Figure 4). A perfectly spherical particle has an S_R value of 1.0; smaller values mean departure from a spherical shape and the theoretical extreme is 0.0.

The roundness of the particle (R_F) of each grain was determined by using the method developed by Dobkins and Folk [30], represented by Eq. (2):

$$R_F = d_k/d_i, \tag{2}$$

where, d_k is the diameter of curvature of the sharpest corner and d_i is the diameter of the inscribed circle (Figure 4). A very well rounded particle has a maximum R_F of 1.0, while an extremely angular particle has a value close to 0.0.

The averages of S_R and R_F values of 120 grains were considered as the representative, presented in Table 3 for each sand sample. As per the roundness classification proposed by Youd [31], Samples A, C, D, F, H, and I contain angular particles, while Samples B, E, and G contain subangular particles. Meanwhile, as per the Russel-Taylor-Pettijohn's roundness chart [32], the S_R values in Table 3 indicate the presence of grains of medium sphericity in the sand samples.

Table 3. Results of the particle shape analyses on the sand samples [22].

Sample	R_F	S_R
A	0.24	0.66
B	0.25	0.67
C	0.19	0.64
D	0.21	0.60
E	0.32	0.65
F	0.20	0.62
G	0.30	0.61
H	0.18	0.63
I	0.21	0.67

2.5. Testing methodology

A 100 kN load cell capacity compression testing machine supplied by Humboldt, USA, was used in this study. The surface area of the plunger is 19.35 cm^2 with the penetration rate of 1.27 mm/min. A 60 kN load cell, attached to a digital readout unit, was utilized for recording the load P transmitted to the sample. Before loading the sample, silicon grease was applied on the two pistons to minimize side friction. The sample was dynamically compacted into the CBR mold in three layers to obtain a certain density. Samples B, E, and H were tested at six different densities; meanwhile, Samples A, C, D, G, and I were tested at seven different densities; and Sample F was tested at eight different densities. For each density tested in each sample, two specimens having diameter of 152 mm, and length of 127 mm were prepared at the same density and at the optimum water contents listed in Table 1 for each sample. After preparation, curing was not applied to the specimens and CBR tests were then carried out on the specimens according to Turkish Standards (TS 1900-2) [33]. Then, the CBR values of the specimens were obtained. Finally, the average value of two tests at the same density was computed and taken as the CBR value of the sample at this density for evaluation of the test results.

3. Results and discussion

The CBR values of the individual specimens obtained for each sand sample were plotted against dry density (ρ_{dry}) to determine the CBR versus ρ_{dry} relationship. The typical CBR versus ρ_{dry} behavior was then obtained as given in Figure 5 for Sample A. The data trends were similar for all samples, indicating the existence of a linear relationship between the CBR and ρ_{dry}. This observation agrees with the past research (e.g., [34-37]). Table 4 summarizes the equations

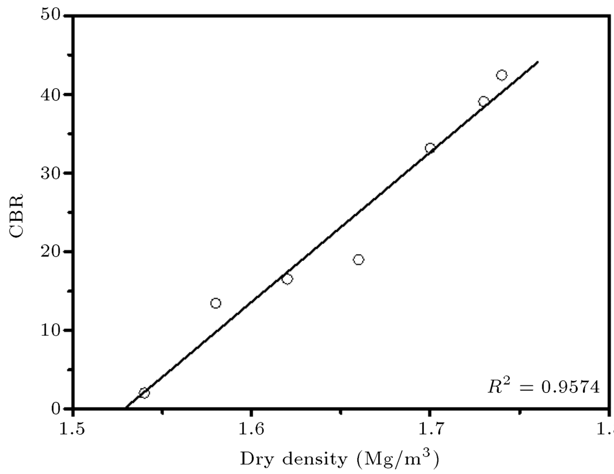

Figure 5. The typical CBR versus dry density behavior of Sample A [22].

Table 4. The equations obtained from the correlations of CBR to ρ_{dry} for each sand sample [22].

Sample	Equation	r	Equation no.
A	CBR = 190.46* ρ_{dry} -291.14	0.978	(3)
B	CBR = 135.17* ρ_{dry} -193.90	0.922	(4)
C	CBR = 74.07* ρ_{dry} -142.23	0.979	(5)
D	CBR = 127.27* ρ_{dry} -181.39	0.928	(6)
E	CBR = 172.23* ρ_{dry} -250.63	0.905	(7)
F	CBR = 70.77* ρ_{dry} -112.40	0.962	(8)
G	CBR = 155.40* ρ_{dry} -283.23	0.968	(9)
H	CBR = 141.43* ρ_{dry} -235.64	0.975	(10)
I	CBR = 157.58* ρ_{dry} -237.84	0.956	(11)

obtained from the correlations of the CBR to ρ_{dry} for each sand sample. In Eqs. (3) to (11) in Table 4, r is the coefficient of correlation and ρ_{dry} is in Mg/m^3. Smith [38] proposed the following guide for the values of $|r|$ between 0.0 and 1.0:

- $|r| \geq 0.8$ Strong correlation exists between the two sets of variables;
- $0.2 < |r| < 0.8$ Correlation exists between the two sets of variables;
- $|r| \leq 0.2$ Weak correlation exists between the two sets of variables.

It can be seen from Table 4 that the r values in Eqs. (3)-(11) are higher than 0.8, which indicate that there is a strong correlation between the CBR and ρ_{dry} for each sand sample.

As mentioned earlier, a CBR value is affected by the type of soil and different soil properties [6]. Therefore, Multiple Regression Analysis (MRA), a statistical technique allowing us to predict someone's score in one variable on the basis of their scores on several other variables [39], was carried out by using a SPSS 13.0 package to correlate the measured CBR values to the soil properties, namely, dry density (ρ_{dry}), relative density (I_D), water content (w), specific gravity (G_s), coefficient of uniformity (C_u), coefficient of curvature (C_c), and particle shape (R_F and S_R). The MRA yielded the following correlations:

$$\text{CBR} = -34.255 + 30.622\rho_{dry} \quad r = 0.556, \tag{12}$$

$$\text{CBR} = -11.876 + 0.520 I_D \quad r = 0.807, \tag{13}$$

$$\text{CBR} = -18.457 + 0.523 I_D + 0.625w \quad r = 0.822, \tag{14}$$

$$\text{CBR} = -41.017 + 30.890\rho_{dry} + 0.612w \quad r = 0.577, \tag{15}$$

$$\text{CBR} = -22.432 + 50.848\rho_{dry} + 1.187w - 20.590G_s \quad r = 0.686, \tag{16}$$

$$\text{CBR} = -50.044 + 0.557I_D + 0.340w + 11.303G_s \quad r = 0.868, \tag{17}$$

$$\text{CBR} = -37.894 + 0.219w + 12.399G_s + 0.622I_D - 15.994C_c \quad r = 0.918, \tag{18}$$

$$\text{CBR} = -51.002 + 0.119w + 13.891G_s + 0.604I_D - 2.360C_u \quad r = 0.895, \tag{19}$$

$$\text{CBR} = -15.879 + 1.167w - 21.244G_s + 52.118\rho_{dry} - 6.414C_c \quad r = 0.697, \tag{20}$$

$$\text{CBR} = -23.966 + 1.059w - 24.902G_s + 66.011\rho_{dry} - 4.008C_u \quad r = 0.763, \tag{21}$$

$$\text{CBR} = -33.229 + 0.300w + 11.344G_s + 0.618I_D - 21.440C_c + 1.302C_u \quad r = 0.920, \tag{22}$$

$$\text{CBR} = -91.597 + 0.835w - 32.817G_s + 101.814\rho_{dry} + 61.263C_c - 17.173C_u \quad r = 0.894, \tag{23}$$

$$\text{CBR} = 25.086 - 15.905R_F \quad r = 0.051, \tag{24}$$

$$\text{CBR} = -13.173 + 54.274S_R \quad r = 0.096, \tag{25}$$

$$\text{CBR} = -10.886 - 18.989R_F + 57.566S_R \quad r = 0.114, \tag{26}$$

$$\text{CBR} = -50.400 + 0.588I_D + 3.784R_F + 51.379S_R \quad r = 0.794, \tag{27}$$

$$\text{CBR} = -8.883 + 0.424w + 11.043G_s + 0.622I_D - 22.285C_c + 0.709C_u - 38.146R_F - 21.070S_R \quad r = 0.925. \tag{28}$$

In Eqs. (12) to (28), r is the coefficient of correlation, ρ_{dry} is in Mg/m^3, and I_D and w are in %.

It can be seen from Eqs. (12) to (28) that the r values in Eqs. (13), (14), (17), (18), (19), (22), (23), and (28) are higher than 0.8, which indicate that there is a strong correlation between the CBR and the soil

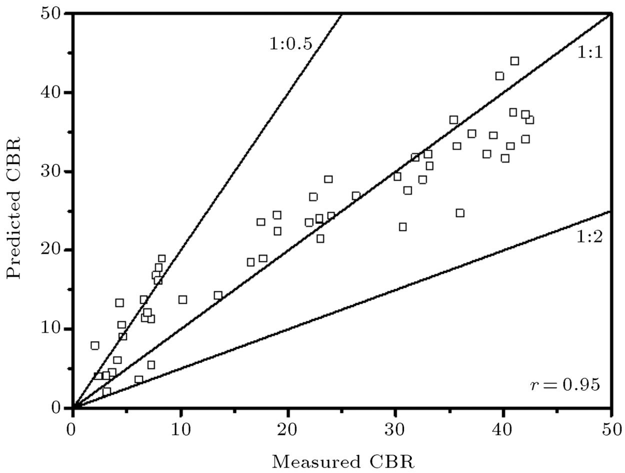

Figure 6. Comparison of experimentally obtained and computed values of CBR.

properties. It can be also noticed from Eqs. (12) to (28) that Eq. (28) reveals the highest correlation coefficient of $r = 0.925$, indicating the strong correlation between the CBR and the soil properties (I_D, w, G_s, C_u, and C_c) and particle shape (R_F and S_R). Therefore, Eq. (28) alone was taken into account for the rest of the study.

The computed CBR values from Eq. (28) are compared with experimentally obtained CBR values in Figure 6. The solid diagonal line in Figure 6 represents a perfect prediction line. The lower line represents a 100% overprediction bound and the upper line represents a 50% under prediction bound. Approximately 80% of the predictions fall onto or are very close to the 1:1 line and approximately 87% of the predictions fall between these two prediction lines. The high coefficient of correlation ($r = 0.925$) indicates a strong correlation between the computed and the measured CBR values. Therefore, it is expected that Eq. (28) can be used to estimate the CBR value of sands from the soil properties (I_D, w, G_s, C_u, and C_c) and particle shape (R_F and S_R) when CBR measurements are not available.

A paired t-test, a statistical test, utilizes the mean of the difference between the observations in one group and the matched observations in the other group. A paired t-test is carried out to determine if there is a significant difference between two observations. A paired t-test result can be expressed in terms of a p-value, which represents the weight of evidence for rejecting the null hypothesis [40]. The null hypothesis is the equality of mean of difference between comparisons [41]. The null hypothesis can be rejected, that is, the mean of difference between comparisons is significant, if the p-value is less than the selected significance level [41]. A significance level of 0.05 is used for all paired t-tests [41]. Thus, $p > 0.05$ meant that there was not a meaningful difference and $p < 0.05$ meant that there was a meaningful difference [42]. In this study, a paired t-test was performed by using the SPSS 13.0 package to look for a statistically significant difference between calculated and predicted CBR values. p-value was found as 0.915, indicating that no significant difference in the CBR values was observed between the calculated and predicted values.

The coefficient of correlation between the measured and the predicted values is a good indicator of the prediction of the model [43]. In this study, different performance indices, namely, variance, VAF, represented by Eq. (29), the Root Mean Square Error, RMSE, represented by Eq. (30), and Mean Absolute Error, MAE, represented by Eq. (31), were also computed to check the performance of the prediction capacity of predictive model (Eq. (28)) developed in the study, as employed by past researchers (e.g. [44-54]).

$$\mathrm{VAF} = \left[1 - \frac{var(y - \hat{y})}{var(y)}\right] \times 100, \tag{29}$$

$$\mathrm{RMSE} = \sqrt{\frac{1}{N}\sum_{i=1}^{N}(y_i - \hat{y}_i)^2}, \tag{30}$$

$$\mathrm{MAE} = \frac{1}{N}\sum_{i=1}^{N}|y_i - \hat{y}_i|, \tag{31}$$

where, var denotes the variance, y is the measured value, $\hat{y}$ is the predicted value, and N is the number of the sample. If VAF is 100% and RMSE and MAE are 0, the model is considered as excellent.

The performance indices calculated for the Eq. (28), suggested for the prediction of CBR, are presented in Table 5. Eq. (28), derived from the samples used in this study, performs well with an acceptable accuracy based on the performance indices in Table 5.

Additionally, a graph between the Scaled Percent Error, SPE, (as given by Eq. (33) and used by Kanibir et al. [55], Erzin et al. [56], and Erzin and Cetin [51]), and the cumulative frequency was plotted, as shown in Figure 7, for the model (Eq. (28)) proposed for prediction of the CBR to examine the performance of the model.

$$\mathrm{PE} = \frac{(\mathrm{CBR}_P - \mathrm{CBR}_m)}{((\mathrm{CBR}_m)_{\max} - (\mathrm{CBR}_m)_{\min})}, \tag{32}$$

where, CBR_P and CBR_m are the predicted and the measured CBR values and $(\mathrm{CBR}_m)_{\max}$ and

Table 5. Performance indices of the developed MR model.

r (%)	RMSE	MAE	VAF (%)
95.0	4.07	5.02	87.12

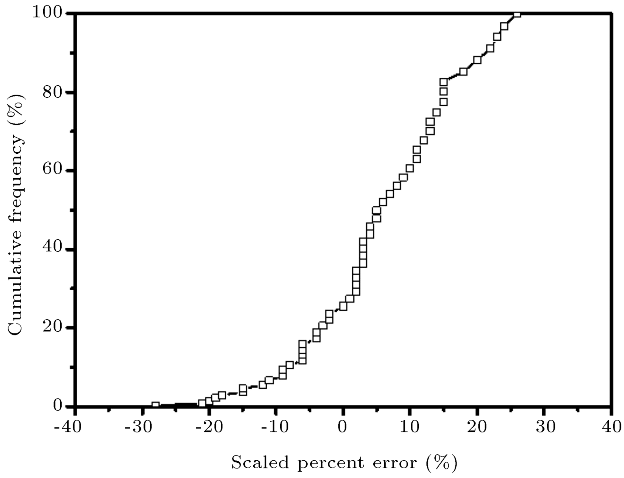

Figure 7. The relationship between the scaled percent error and cumulative frequency.

$(\mathrm{CBR}_m)_{\min}$ are the maximum and minimum measured CBR values, respectively. It can be observed from Figure 7 that about 87% of CBR values predicted by the model developed in this study fall into ±20% of the SPE, indicating a perfect estimate of the CBR value by the model. From here, it can be concluded that the CBR value of the sands used in this study could be predicted from the soil properties (I_D, w, G_s, C_u, and C_c) and particle shape (R_F and S_R) using Eq. (28), with acceptable accuracy when the CBR measurements are not available. Also, it must be considered that the equation proposed in this paper was obtained from the sands having sphericity range of 0.60 to 0.67, and roundness range of 0.18 to 0.32. Therefore, for wider and generalized application of Eq. (28), the formulae would have to be tested over a data set with a large range of sphericity and angularity.

4. Conclusions

In this study, the factors affecting the CBR value of Aegean sands have been investigated. For this purpose, Aegean sands were collected from nine different locations in Manisa, Turkey. Mineralogical, particle shape and size, specific gravity, and the CBR tests were performed on the samples of sands. The influences of dry density, relative density, water content, particle shape, and particle size on the CBR value were examined. It has been observed that the CBR value increases with dry density for each sample. In addition, an MR equation was proposed for predicting the CBR value of sands based on their particle shape, specific gravity, coefficient of uniformity, coefficient of curvature, relative density, and water content. The computed values from the equation were found to be in good agreement with those obtained from the experimental values.

In addition, several performance indices, such as coefficient of correlation, variance, mean absolute error, mean squared error, and scaled percentage error, were used to assess the performance of the MR model proposed for estimation of the CBR. The study demonstrates that the MR model is able to predict the CBR values of the sands used in this study. Thus, MR model can be used to predict the CBR values of sands as an inexpensive substitute for laboratory testing, quite easily and efficiently.

Acknowledgments

The authors thank Prof. Dr. Huseyin Yalcin (Cumhuriyet University, Sivas, Turkey) for his evaluation of XRD diffractograms.

References

1. Nguyen, B.T. and Mohajerani, A. "Prediction of California bearing ratio from physical properties of fine-grained soils", *World Academy of Science, Engineering and Technology International Journal of Civil, Structural, Construction and Architectural Engineering*, **9**(2), pp. 136-141 (2015).

2. Chegenizadeh, A. and H.R. Nikraz. "CBR test on reinforced clay", In *The 14th Pan-American Conference on Soil Mechanics and Geotechnical Engineering (PCSMGE), the 64th Canadian Geotechnical Conference (CGC)*, Oct. 2, Toronto, Ontario, Canada: Canadian Geotechnical Society (2011).

3. Zumrawi, M.M. "Prediction of CBR from index properties of cohesive soils", *Advances in Civil Engineering and Building Materials*, Edited by Shuenn-Yih Chang, Suad Khalid Al Bahar, and Jingying Zhao, CRC Press, pp. 561-565 (2012).

4. Day, W.R., *Soil Testing Manual: Procedures, Classification Data, and Sampling Practices*, USA, p. 619 (2001).

5. Yildirim, B. and Gunaydin, O. "Estimation of California bearing ratio by using soft computing systems", *Expert Syst. Appl.*, **38**, pp. 6381-6391 (2011).

6. Zumrawi, M.M. "Prediction of in-situ CBR of subgrade cohesive soils from dynamic cone penetrometer and soil properties", *IACSIT International Journal of Engineering and Technology*, **6**(5), pp. 439-442 (2014).

7. Black, W.P.M. "A method of estimating the CBR of cohesive soils from plasticity data", *Geotechnique*, **12**, pp. 271-272 (1962).

8. De Graft-Johnson, J.W.S. and Bhatia, H.S. "The engineering characteristics of the lateritic gravels of Ghana", In *Proceedings of 7th International Conference on Soil Mechanics and Foundation Engineering*, **2**, Mexico, August 28-29. Bangkok: Asian Institute of Technology, pp. 13-43 (1969).

9. Agarwal, K.B. and Ghanekar, K.D. "Prediction of CBR from plasticity characteristics of soil", *Proceeding of 2nd South-East Asian Conference on Soil Engineering*, Singapore, June 11-15, Bangkok: Asian Institute of Technology, pp. 57–576 (1970).

10. Linveh, M. "Validation of correlations between a number of penetration test and in situ California bearing ratio test", *Transport. Res. Rec. 1219*, pp. 56-67 (1989).

11. Stephens, D.J. "Prediction of the California bearing ratio", *J. Civil Eng. S Afr.*, **32**(12), pp. 523-527 (1990).

12. Al-Refeai, T. and Al-suhaibani, A. "Prediction of CBR using dynamic cone penetrometer", *King Saud U J., Eng. Sci.*, **9**(2), pp. 191-204 (1997).

13. Satyanarayana Reddy, C.N.V. and Pavani, K. "Mechanically stabilised soils-regression equation for CBR evaluation", *Proceedings of Indian Geotechnical Conference*, Chennai, India, Dec. 14-16, pp. 731-734 (2006).

14. Kin, M.W. "California bearing ratio correlation with soil index properties", Master Degree Project, Faculty of Civil Engineering, University Technology Malaysia (2006).

15. Vinod, P. and Reena, C. "Prediction of CBR value of lateritic soils using liquid limit and gradation characteristics data", *Highway Res J., IRC*, **1**(1), pp. 89-98 (2008).

16. Gunaydin, O. "Estimation of compaction parameters by using statistical analyses and artificial neural networks", *Environ Geol.*, **57**, pp. 203-215 (2009).

17. Patel, S.R. and Desai, M.D. "CBR predicted by index properties for alluvial soils of South Gujarat", *Proceedings of Indian Geotechnical Conference*, Dec. 16-18, pp. 79-82, India (2010).

18. Taskiran, T. "Prediction of California bearing ratio (CBR) of fine grained soils by AI methods", *Adv. Eng. Softw.*, **41**(6), pp. 886-892 (2010).

19. Venkatasubramanian, C. and Dhinakaran, G. "ANN Model for predicting CBR from Index properties of soils", *Int. J. Civil Struct. Eng.*, **2**(2), pp. 605-611 (2011).

20. Alawi, M.H. and Rajab, M.I. "Prediction of California bearing ratio of subbase layer using multiple linear regression models", *Road Mater Pavement Design*, **14**(1), pp. 211-219 (2013).

21. Ramasubbarao, G.V. and Siva Sankar, G. "Predicting soaked CBR value of fine grained and compaction characteristics", *Jordan J. Civil Eng.*, **7**(3), pp. 354-360 (2013).

22. Turkoz, D. "Investigations on the factors influencing the California bearing ratio value of some Aegean sands", MSc. Thesis, Celal Bayar University Manisa, Turkey (2014) (In Turkish).

23. ASTM D 422-63 "Standard test method for particle size analysis of soils" *Annual Book of ASTM Standards, ASTM*, West Conshohocken, PA, USA, 04.08, pp. 10-16 (1994).

24. TS 1900-1 (Turkish Standard), *Methods of Testing Soils for Civil Engineering Purposes in the Laboratory - Part 1: Determination of Physical Properties* (2006).

25. BS1377, *Soils for Civil Engineering Purposes; Part 4: Compaction-Related Tests*, British Standards Institution (1990).

26. Blatt, H., Middleton, G. and Murray, R., *Origin of Sedimentary Rocks*, Prentice Hall Inc., Englewood Cliffs (1971).

27. Shahu, J.T. and Yudhbir, "Model tests on sands with different angularity and mineralogy", *Soils Found.*, **38**(4), pp. 151-158 (1998).

28. Wadell, H. "Volume, shape, and roundness of rock particles", *J Geol.*, **40**, pp. 443-451 (1932).

29. Riley, N.A. "Projection sphericity", *Journal of Sedimentary Petrology*, **1**, pp. 94-97 (1941).

30. Dobkins, J.E. and Folk, R.L. "Shape development on Tahiti-Nui", *J. Sediment Petrol.*, **40**, pp. 1167-1203 (1970).

31. Youd, T.L. "Factors controlling maximum and minimum densities of sands", *ASTM Special Technical Publication*, **523**, pp. 98-112 (1973).

32. Muller, G. "Methods in sedimentary petrology", *Section on: Degree of Roundness According to Russel-Taylor-Pettijohn (after Schneiderhohn)*, pp. 100-101, Hafner, N.Y. (1967).

33. TS 1900-2 (Turkish Standard), *Methods of Testing Soils for Civil Engineering Purposes in the Laboratory - Part 2: Determination of Mechanical Properties* (2006).

34. Doshi, S.N., Mesdary, M.S. and Guirguis, H.R. "Statistical study of laboratory CBR for Kuwaiti soils", In *Fourth Conference of the Road Engineering Association of Asia and Australasia*, **2**, Jakarta, pp. 43-51 (1983).

35. Taskiran, T. "Prediction of California bearing ratio (CBR) of fine grained soils by AI methods", *Adv. Eng. Softw.*, **41**(6), pp. 886-892 (2010).

36. Shirur, N.B. and Hiremath, S.G. "Establishing relationship between CBR value and physical properties of soil", *IOSR Journal of Mechanical and Civil Engineering*, **11**(5), pp. 26-30 (2014).

37. Leung, G.L.M., Wong, A.W.G. and Wang, Y.H. "Prediction of resilient modulus of compacted saprolitic soils by CBR approach for road pavement subgrade: A re-examination", *International Journal of Pavement Engineering*, **14**(4), pp. 403-417 (2013).

38. Smith, G.N., *Probability and Statistics in Civil Engineering: An Introduction*, Collins, London (1986).

39. Auli, K.A., Parsinejad, M. and Rahmani, B. "Estimation of saturation percentage of soil using multiple regression, ANN, and ANFIS techniques", *J. Comput. Inform. Sci.*, **2**(3), pp. 127-136 (2009).

40. Ott, L.R. and Longnecker, M., *An Introduction to Statistical Methods and Data Analysis*, 5th Edn., Duxbury, Pacific Grave, California (2001).

41. Ceylan, H., Gopalakrishnan, K. and Kim, S. "Soil stabilization with bioenergy coproduct", *Transportation Research Record. No. 2186*, Washington D.C., pp. 30-137 (2010).

42. Tüysüz, C., *The Effect of the Virtual Laboratory on the Students' Achievement and Attitude in Chemistry*, *IOJES*, **2**(1), pp. 37-53 (2010).

43. Gokceoglu, C. and Zorlu, K. "A fuzzy model to predict the uniaxial compressive strength and the modulus of elasticity of a problematic rock", *Eng. Appl. Artif. Intel.*, **17**(1), pp. 61-72 (2004).

44. Erzin, Y. "Artificial neural networks approach for swell pressure versus soil suction behavior", *Can. Geotech. J.*, **44**(10), pp. 1215-1223 (2007).

45. Erzin, Y., Rao, B.H. and Singh, D.N. "Artificial neural networks for predicting soil thermal Resistivity", *Int. J. Therm. Sci.*, **47**, pp. 1347-1358 (2008).

46. Erzin, Y., Gumaste, S.D., Gupta, A.K. and Singh, D.N. "ANN models for determining hydraulic conductivity of compacted fine grained soils", *Can. Geotech. J.*, **46**, pp. 955-968 (2009).

47. Erzin, Y., Rao, B.H., Patel, A., Gumaste, S.D., Gupta, A.K. and Singh, D.N. "Artificial neural network models for predicting of electrical resistivity of soils from their thermal resistivity", *Int. J. Therm. Sci.*, **49**, pp. 118-130 (2010).

48. Erzin, Y. and Gunes, N. "The prediction of swell percent and swell pressure by using neural networks", *Math. Comput. Appl.*, **16**(2), pp. 425-436 (2011).

49. Erzin, Y. and Cetin, T. "The use of neural networks for the prediction of the critical factor of safety of an artificial slope subjected to earthquake forces", *Sci Iran.*, **19**(2), pp. 188-194 (2012).

50. Erzin, Y. and Cetin, T. "The prediction of the critical factor of safety of homogeneous finite slopes using neural networks and multiple regressions", *Comput Geosci.*, **51**, pp. 305-313 (2013).

51. Erzin, Y. and Cetin, T. "The prediction of the critical factor of safety of homogeneous finite slopes subjected to earthquake forces using neural networks and multiple regressions", *Int. J. Geomech. Eng.*, **6**(1), pp. 1-15 (2014).

52. Erzin, Y. and Gul, T. "The use of neural networks for the prediction of the settlement of pad footings on cohesionless soils based on standard penetration test", *Int. J. Geomech. Eng.*, **5**(6), pp. 541-564 (2013).

53. Erzin, Y. and Gul, T. "The use of neural networks for the prediction of the settlement of one-way footings on cohesionless soils based on standard penetration test", *Neural Comput. Applic.*, **24**, pp. 891-900 (2014).

54. Erzin, Y., Ecemis, N. "The use of neural networks for CPT-based liquefaction screening", *B. Eng. Geol. Environ.*, **74**, pp. 103-116 (2015).

55. Kanibir, A., Ulusay, R. and Aydan, Ö. "Liquefaction-induced ground deformations on a lake shore (Turkey) and empirical equations for their prediction", *IAEG2006*, paper 362 (2006).

56. Erzin, Y., Patel, A., Singh, D.N., Tiga, M.G., Yılmaz, I. and Srinivas, K. "Investigations on factors influencing the crushing strength of some Aegean sands", *B. Eng. Geol. Environ.*, **71**, pp. 529-536 (2012).

Biographies

Yusuf Erzin is Associate Professor in the Department of Civil Engineering at Celal Bayar University, Manisa, Turkey. He received his BS degree in Civil Engineering from Selçuk University, Konya, Turkey, and his MS and PhD degrees in Civil Engineering from Middle East Technical University, Ankara, Turkey. His research interests include artificial neural networks, swelling soils, slope stability, and crushing strength of sands. He has published 20 papers in many International Journals.

Deniz Türköz received MS and BS degrees in Civil Engineering from Celal Bayar University, Manisa, Turkey. She is currently working in a public agency.

Yesim Tuskan is Research Assistant in the Department of Civil Engineering at Celal Bayar University, Manisa, Turkey. She received BS and MS degrees in Civil Engineering from Celal Bayar University, Manisa, Turkey. She is currently a PhD student in the same university. Her research interests include computer programming, artificial neural networks, slope stability.

Isik Yılmaz is lecturer and scientist at Cumhuriyet University in Turkey and a specialist in the subjects of engineering geology, rock mechanics, soil mechanics, GIS, soft computing techniques in rock/soil parameter estimation and hazard/susceptibility mapping of landslide and liquefaction, and topographical deformations depending on underground mining. He has 5 books and more than 100 papers published in many international Journals. He is Editor and/or Editorial board member of many International Journals.